Sharp Tunneling Peaks in a Parametric Oscillator: Quantum Resonances Missing in the Rotating Wave Approximation

V. Peano,[1] M. Marthaler,[2] and M. I. Dykman[1]

[1]*Department of Physics and Astronomy, Michigan State University, East Lansing, Michigan 48824, USA*

[2]*Institut für Theoretische Festkörperphysik and DFG-Center for Functional Nanostructures (CFN), Karlsruhe Institute of Technology, D-76128 Karlsruhe, Germany*

(Received 21 March 2012; published 27 August 2012)

We describe a new mechanism of tunneling between period-two vibrational states of a weakly nonlinear, parametrically modulated oscillator. The tunneling results from resonant transitions induced by the fast oscillating terms conventionally disregarded in the rotating wave approximation (RWA). The tunneling amplitude displays resonant peaks as a function of the modulation frequency; near the maxima it is exponentially larger than the RWA tunneling amplitude.

DOI: 10.1103/PhysRevLett.109.090401 PACS numbers: 03.65.Xp, 05.60.Gg, 42.50.Pq, 74.78.Na

Many systems of current interest can be modeled by modulated nonlinear quantum oscillators. Examples range from Josephson junction based systems [1] to optical cavity modes [2], electrons in a Penning trap [3], and opto- and nanomechanical systems [4]. The oscillator dynamics is often characterized by well-separated time scales: the reciprocal eigenfrequency ω_0^{-1} and a much longer time related to the vibration decay and nonlinearity. A standard approach to the analysis of the dynamics is based on the rotating wave approximation (RWA), where one separates slow variables, like the vibration amplitude and the slow part of the phase, and disregards the effect of fast oscillating terms on their evolution.

An important quantum effect in modulated systems is dynamical tunneling [5]. It can be understood for a parametric oscillator, which is excited by modulation at frequency ω_F close to $2\omega_0$. Classically, a weakly nonlinear oscillator can have two states of vibrations at frequency $\omega_F/2$, which have the same amplitudes and differ in phase by π [6]. Quantum fluctuations cause tunneling between these states [7,8]. Similar tunneling, which should be distinguished from dissipative switching [9,10], is known also for other types of vibration bistability [11].

In this Letter, we show that the tunneling rate of a parametrically modulated oscillator can be exponentially increased by processes caused by the fast oscillating terms $\propto \exp(\pm in\omega_F t)$, $(n = 1, 2, \ldots)$ disregarded in the RWA. This happens where the difference of the appropriate eigenvalues of the RWA Hamiltonian becomes close to $n\hbar\omega_F$. The level configuration is of Λ-type. The two lowest RWA levels are degenerate (disregarding tunneling), with the wave functions localized near the period-two vibrational states, whereas the upper-level state is delocalized, see Fig. 1. The three states are resonantly mixed by the fast-oscillating non-RWA terms. The associated breakdown of the RWA is a purely quantum effect with no classical counterpart.

The tunneling enhancement we consider is somewhat reminiscent of photon-assisted tunneling from a potential well, which is now broadly used in quantum information processing [12]. There, photon absorption resonantly accelerates tunneling decay if the photon energy $\hbar\omega_F$ coincides with the intrawell level spacing, since the decay rate of the excited state largely exceeds that of the ground state. In contrast to systems displaying photon-assisted tunneling, a parametric oscillator is bistable due to the modulation, which forms the very barrier for tunneling in phase space. This leads to a different physics and requires a different description.

We study moderately strong resonant modulation where the nonlinear part of the oscillator vibration energy remains small compared to the harmonic part. This makes the oscillator different from modulated strongly nonlinear systems where much attention has attracted chaos-assisted [13] and nonlinear resonance-assisted tunneling [14], see Supplemental Material [15]. For the rate of tunneling between the vibrational states to be small, the effective

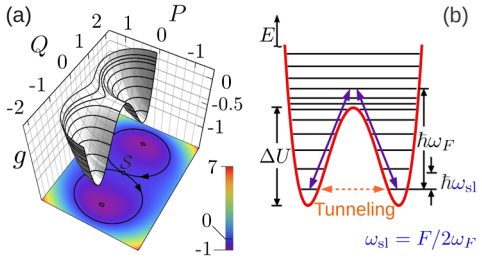

FIG. 1 (color online). (a) The dimensionless RWA Hamiltonian $g(Q, P)$, Eq. (3), for $\mu = 0.95$. The minima of $g(Q, P)$ correspond to the parametrically excited vibrational states, in the presence of weak dissipation. (b) The cross section $g(Q, P = 0)$ with a sketch of RWA quasienergy levels; the arrows indicate resonant transitions due to the fast-oscillating corrections to the RWA. Also indicated are the typical energy scales.

RWA tunneling barrier ΔU should largely exceed the RWA level spacing $\hbar\omega_{\rm sl}$; frequency $\omega_{\rm sl}$ characterizes the oscillator dynamics in the rotating frame, $\omega_{\rm sl} \ll \omega_F \approx 2\omega_0$. The ratio $\Delta U/\hbar\omega_F$ can be arbitrary, it does not emerge in the RWA. We will be interested in the case where $\Delta U \sim \hbar\omega_F$. In this case the effect of resonant admixture of the RWA states by the non-RWA interaction, is most pronounced, see Fig. 1.

For $\omega_F \gg \omega_{\rm sl}$, the states resonantly mixed by the non-RWA terms in the oscillator Hamiltonian overlap very weakly. We develop a method that allows us to calculate the relevant exponentially small matrix elements and to show that they are nevertheless sufficiently large to lead to exponential resonant enhancement of tunneling.

The Hamiltonian of a parametrically modulated oscillator with coordinate q and momentum p reads

$$H(t) = \frac{p^2}{2} + \frac{1}{2}q^2[\omega_0^2 + F\cos(\omega_F t)] + \frac{\gamma}{4}q^4. \quad (1)$$

We assume that the modulation amplitude F and the nonlinearity are comparatively small, $F,\ \gamma\langle q^2\rangle \ll \omega_0^2$, and the modulation frequency ω_F is close to resonance, $|\omega_F - 2\omega_0| \ll \omega_0$; for concreteness we set $F,\ \gamma > 0$. Of primary interest is the range of the modulation parameters F and ω_F where, in the presence of weak damping, the oscillator has two almost sinusoidal stable classical vibrational states with frequency $\omega_F/2$ [6].

To study the oscillator dynamics, we switch to the rotating frame using a standard transformation $U(t) = \exp[-i\omega_F\hat{a}^\dagger\hat{a}t/2]$ and introduce dimensionless slow variables Q and P, $U^\dagger qU = C[P\cos\omega_F t/2 - Q\sin\omega_F t/2]$ and $U^\dagger pU = -(\omega_F/2)C[P\sin\omega_F t/2 + Q\cos\omega_F t/2]$. Here $\hat{a}$ and $\hat{a}^\dagger$ are the ladder operators and $C = (2F/3\gamma)^{1/2}$. The Hamiltonian in the rotating frame $\tilde{H} = U^\dagger HU - i\hbar U^\dagger\dot{U}$ reads

$$\tilde{H} = (F^2/6\gamma)[g(Q,P) + h(Q,P,t)]. \quad (2)$$

The dimensionless operator

$$\hat{g} = \frac{1}{4}(Q^2+P^2)^2 + \frac{1}{2}(1-\mu)P^2 - \frac{1}{2}(1+\mu)Q^2 \quad (3)$$

is independent of time [8]. In contrast, the operator

$$\hat{h} = h_1(Q,P)e^{-i\omega_F t} + h_2(Q,P)e^{-2i\omega_F t} + \text{H.c.}$$

is fast oscillating; $h_{1,2}$ are fourth order polynomials in Q, P, they do not contain small parameters and are given explicitly in the Supplemental Material [15]. Functions $g(Q,P)$ and $h(Q,P)$ are symmetric with respect to inversion $(Q,P) \to (-Q,-P)$ due to the periodicity of $H(t)$. They depend on a single dimensionless parameter μ,

$$\mu = [(\omega_F/2) - \omega_0]/\omega_{\rm sl}, \qquad \omega_{\rm sl} = F/2\omega_F. \quad (4)$$

We disregard corrections $\sim\omega_{\rm sl}/\omega_F$.

The commutation relation for the dimensionless coordinate Q and momentum P is

$$[Q,P] = i\lambda, \qquad \lambda = 3\gamma\hbar/(F\omega_F), \quad (5)$$

where λ is the dimensionless Planck constant. We assume that $\lambda \ll 1$. Then quantum fluctuations are small on average.

From Eq. (2), the Schrödinger equation in dimensionless time $\tau = t\omega_{\rm sl}$ is $i\lambda\partial_\tau\Psi = (\hat{g} + \hat{h})\Psi$. Since $\hat{h}$ is periodic in time, this equation has Floquet solutions $\Psi_\epsilon(\tau + \tau_h) = \exp(-i\epsilon\tau_h/\lambda)\Psi_\epsilon(\tau)$. They define the dimensionless quasienergies ϵ [$\tau_h = 2\pi\omega_{\rm sl}/\omega_F \ll 1$].

In the RWA, the fast oscillating term $\hat{h}$ is disregarded. Then operator $\tilde{H}$ becomes time-independent. The dimensionless Hamiltonian $g(Q,P)$, Eq. (3), is shown in Fig. 1. It is not a sum of the kinetic and potential energy. For $|\mu| < 1$, $g(Q,P)$ has two symmetrically located minima, $g_{\rm min} = -(1+\mu)^2/4$, and a saddle point, $g_S = 0$. In the presence of weak dissipation, the minima correspond to the period-2 vibrational states in the laboratory frame, which have equal amplitude and opposite phase. The barrier height between the states is $\Delta U = (F^2/6\gamma)(g_S - g_{\rm min})$.

The eigenvalues g_m of $\hat{g}$ give dimensionless quasienergies ϵ_m in the RWA. For $\lambda \ll 1$ each well of $g(Q,P)$ in Fig. 1 contains many levels, $\propto 1/\lambda$. Because the wells are symmetric, the intrawell states are degenerate in the neglect of tunneling. With account taken of tunneling, the eigenstates $\psi_n(Q)$ of $\hat{g}$ are even or odd in Q, and index n is used to enumerate these exact eigenstates. The dimensionless RWA tunnel splitting δg_0 between the lowest-g states was considered earlier [7,8]. It is exponentially small, $|\log\delta g_0| \propto 1/\lambda$, and δg_0 oscillates with μ/λ [8].

The oscillating term $\hat{h}$ in the Hamiltonian (2) mixes RWA eigenstates. For remote states, the mixing is exponentially weak. However, it may become important where $\hbar\omega_F$ is close to the distance between the RWA levels, as it provides a new route for interwell transitions. Consider state ψ_n above the barrier top with dimensionless quasienergy g_n and the two lowest states $\psi_0^{(l)}$ and $\psi_0^{(r)}$ in the left and right wells of $g(Q,P)$ with quasienergy g_0 in the neglect of tunneling, see Fig. 1(b). The dimensionless detuning between the interlevel distance and $\hbar\omega_F$ is $\Delta = \lambda^{-1}(g_n - g_0) - (\omega_F/\omega_{\rm sl})$. If $|\Delta| \ll 1$, transitions $\psi_0^{(l,r)} \to \psi_n$ are resonant. The matrix elements $\langle\psi_n|h_1|\psi_0^{(l)}\rangle$ and $\langle\psi_n|h_1|\psi_0^{(r)}\rangle$ are equal for a symmetric $\psi_n(Q)$ or have opposite signs for an antisymmetric $\psi_n(Q)$; we denote their absolute value by $h_{\rm res}$. The amplitudes of resonantly coupled states $\psi_n(Q)$, $\psi_0^{(l,r)}(Q)$ oscillate at dimensionless frequencies

$$\nu_\pm = [(\Delta^2 + 8\lambda^{-2}h_{\rm res}^2)^{1/2} \pm |\Delta|]/2. \quad (6)$$

From Eq. (6), $\nu_\pm \approx \sqrt{2}h_{\rm res}/\lambda$ for good resonance, $\lambda|\Delta|/h_{\rm res} \ll 1$. In the dispersive regime, $\lambda|\Delta|/h_{\rm res} \gg 1$, interwell oscillations are characterized by frequency $\nu_- \approx 2h_{\rm res}^2/\lambda^2\Delta$. As we show, in both cases ν_- can be exponentially larger than the dimensionless RWA tunneling frequency $\delta g_0/\lambda$, which was disregarded in Eq. (6).

The relevant matrix elements of $\hat{h}$ can be found using the WKB approximation, in the spirit of Ref. [16]. Interestingly, taking advantage of the conformal property of classical trajectories for the effective Hamiltonian $\hat{g}$, one can find both the exponent and the prefactor in the matrix elements. For the term $\propto h_1$ in $\hat{h}$, we write

$$\langle \psi_n|\hat{h}_1|\psi_0\rangle = 2\,\mathrm{Re}\int_0^\infty dQ h^+(Q),$$
$$h^+(Q) = \psi_n^+(Q)\hat{h}_1\psi_0(Q), \tag{7}$$

where $\psi_0(Q)$ is one of the two tunnel-split lowest-g states [the symmetric or antisymmetric combination of $\psi_0^{(l)}(Q)$ and $\psi_0^{(r)}(Q)$]; $\psi_n(Q)$ has the same parity as ψ_0. Here, we provide results for underbarrier states, $g_n < g_S = 0$, and $\mu < 0$; more details are provided and other cases are discussed in the Supplemental Material [15].

Function $\psi_n^+(Q)$ is an eigenfunction of operator $\hat{g}$ such that $\mathrm{Re}[\psi_n^+(Q)] = \psi_n(Q)$ and, in the classically accessible region of the semiaxis $Q > 0$, see Fig. 1,

$$\psi_n^+(Q) \approx c_n(\partial_P g_n)^{-1/2}\exp[i\lambda^{-1}S_n(Q) + i\pi/4]. \tag{8}$$

Here, $S_n(Q) = \int_{a_R(g_n)}^{Q} P(Q', g_n)dQ'$ is the mechanical action counted off from the right turning point $a_R(g_n)$ and $P(Q, g)$ is the classical momentum,

$$P(Q, g) = \sqrt{\mu - 1 - Q^2 + 2\sqrt{g - g_{\min} - \mu + Q^2}}. \tag{9}$$

In Eq. (8) $\partial_P g_n$ is $\partial_P g$ calculated for $P = P(Q, g_n)$ and $c_n = [\tau_p^{(1)}(g_n)/2]^{-1/2}$, where $\tau_p^{(1)}(g)$ is the period of classical vibrations with quasienergy g.

We shift the integration path in Eq. (7) to the upper half-plane, contour $\mathcal{C}$ in Fig. 2(a). On this contour [16]

$$h^+ \approx [c_n c_0 h_1(Q, -P(Q, g_0))/2\sqrt{\partial_P g_n \partial_P g_0}]$$
$$\times \exp\{i[S_n(Q) - S_0(Q)]/\lambda\}. \tag{10}$$

We then change from integration along $\mathcal{C}$ to integration along the semicircle $\mathcal{C}_{\mathrm{arc}}$ at $|Q| \to \infty$, $\mathrm{Im}\, Q > 0$, and contour $\mathcal{C}'$ that for $\mu < 0$ goes above the real axis from $-\infty$ to $Q = +0$ around the branch cut on the imaginary axis, see Fig. 2(a). We use that the classical trajectories $Q(\tau; g)$ for the Hamiltonian $g(Q, P)$ are expressed in terms of the Jacobi elliptic functions [8]. For each g, this expression provides conformal mapping of the half-plane $\mathrm{Im}\, Q > 0$ (with a branch cut) onto a g-dependent region on the plane of complex time τ. We define $\tau(Q, g)$ as the duration of classical motion from the turning point $a_R(g)$ to Q. Then, for $\mu < 0$ the region on the τ-plane that corresponds to the half-plane $\mathrm{Im}\, Q > 0$ is the interior of a rectangle shown in Fig. 2(b).

Using that $\tau(Q, g) = \partial S/\partial g$, we write the exponent in Eq. (10) as

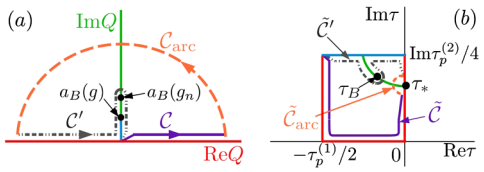

FIG. 2 (color online). (a) The contour of integration $\mathcal{C}$ for calculating the matrix element (7) in the WKB approximation and the auxiliary integration contours for $\mu < 0$; $a_B(g) = i(g - g_{\min} - \mu)^{1/2}$ is the branching point of $P(Q, g)$. (b) Mapping of the half-plane $\mathrm{Im}\, Q > 0$ (with a branch cut) on the interior of a rectangle on the τ-plane for $\mu < 0$ by function $Q(\tau; g)$ that describes the classical Hamiltonian trajectory with given g; $\tau_p^{(1)}$, $\tau_p^{(2)}$, and τ_* are the real and imaginary periods and the pole of $Q(\tau; g)$, respectively. The color coding is the same as in (a). The lines $\tilde{\mathcal{C}}$, $\tilde{\mathcal{C}}_{\mathrm{arc}}$, and $\tilde{\mathcal{C}}'$ are the maps of the corresponding contours in (a). The arc in the upper right corner (green online) is the map of the axis $\mathrm{Im}\, Q$ from $a_B(g)$ to ∞; τ_B is the time for reaching $a_B(g_n)$. The horizontal line $\mathrm{Im}\, \tau = \mathrm{Im}\tau_p^{(2)}/4$ in (b) (blue online) corresponds to the section of the $\mathrm{Im}\, Q$ axis in (a) that goes from $\mathrm{Im}\, Q = 0$ to $\mathrm{Im}\, Q = a_B(g) < a_B(g_n)$. This part of the $\mathrm{Im}\, Q$ axis is shown in blue online.

$$\frac{i}{\lambda}[S_n(Q) - S_0(Q)] = \frac{i}{\lambda}\int_{g_0}^{g_n} dg\,\tau(Q, g). \tag{11}$$

As seen in Fig. 2(b), for any Q on contour $\mathcal{C}_{\mathrm{arc}}$ and any Q' on contour $\mathcal{C}'$, $\mathrm{Im}\tau(Q, g) < \mathrm{Im}\tau(Q', g)$. Therefore, the integral along $\mathcal{C}'$ can be disregarded.

On contour $\mathcal{C}_{\mathrm{arc}}$, $\tau(Q, g)$ is given by the position of the pole $\tau_*(g)$ of function $Q(\tau; g)$ [8], whereas from Eqs. (3) and (9) and the expression for $h_1(Q, -P(Q, g_0))$ (see Supplemental Material [15]) the prefactor in h^+ is $\propto 1/Q$. Then from Eq. (7) for $h_{n0} \equiv \langle \psi_n|\hat{h}_1|\psi_0\rangle$ we obtain

$$h_{n0} \approx \frac{\pi}{3} c_n c_0 \exp\left[-\lambda^{-1}\int_{g_0}^{g_n} dg\,\mathrm{Im}\tau_*(g)\right]. \tag{12}$$

Equation (12) gives the matrix elements of the fast-oscillating field h_1 in the explicit form, including both the exponent and the prefactor. The matrix elements of h_2 are exponentially smaller than those of h_1 and can be disregarded. Equation (12) is in excellent agreement with numerical calculations, see Fig. 3, except for $g_n \to 0$, since Eq. (8) must be modified for such g_n. Numerically, the error is $\lesssim 10\%$ for $|g_n|/\lambda(1 - \mu^2)^{1/2} \gtrsim 0.5$. Equation (12) should also hold for not too large $g_n > 0$, see Supplemental Material [15]. This is fully corroborated by numerical calculations as well.

Expression (12) determines the matrix element $h_{n0} = |h_{n0}|/\sqrt{2}$ in Eq. (6) for the interwell oscillation frequency. One should compare the exponent in Eq. (12) with the RWA tunneling exponent $|\ln\delta g_0|$. The latter is determined by action $S_0(-a_R(g_0))$ for moving under the barrier from one well of $g(Q, P)$ to the other [8]. By symmetry, it is

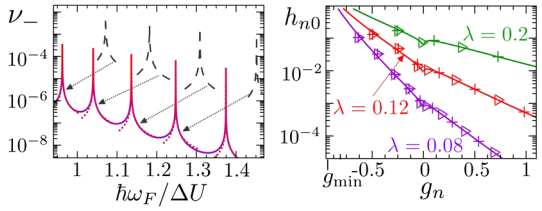

FIG. 3 (color online). Left panel: the scaled tunnel splitting $\nu_- = (\epsilon_1 - \epsilon_0)/\lambda$ for the quasienergy states that maximally overlap with the lowest-g states $(\psi_0^{(l)} \pm \psi_0^{(r)})/\sqrt{2}$ for $\mu = 0.95$ and $\lambda = 0.08$ (for these parameter values, the "direct" tunnel splitting is $\delta g_0/\lambda \approx 0.8 \times 10^{-11}$). The quasienergies $\epsilon_{0,1}$ are obtained numerically from the Schrödinger equation with the full Hamiltonian $H(t)$. The dotted lines show a comparison of the peak shapes with Eq. (12) for renormalized g_n, h_{n0}; the resonating g_n are near the barrier top in Fig. 1, with $n = 14$ for the left peak. The dashed lines show the peaks calculated disregarding the renormalization. Right panel: A comparison of Eq. (12) for h_{n0} calculated as a continuous function of g (the solid lines) with numerical calculations; the triangles and crosses refer to symmetric and antisymmetric states ψ_n. A narrow vicinity of $g_n = 0$, where expression (12) goes to zero as $|\ln g_n|^{-1/2}$ is not shown.

given by twice the real part of Eq. (11) for $g_n = 0$ and $Q = +0$. From Fig. 2(b), $\mathrm{Im}\tau(0, g) = \mathrm{Im}\tau_p^{(2)}(g)/4 > \mathrm{Im}\tau_*(g)$ for $g < 0$. Therefore for $g_n < 0$ not only $|h_{n0}|$, but also $|h_{n0}|^2$ are exponentially larger than δg_0. As shown in Supplemental Material [15], this relation holds also for $\mu > 0$.

Of utmost interest for observing non-RWA tunneling is resonance of $\hbar\omega_F$ with states close to the barrier top in Fig. 1. This is because the matrix element h_{n0} falls down exponentially with increasing g_n. On the other hand, deep inside the wells of $g(Q, P)$, the splitting of the symmetric and antisymmetric states becomes smaller than h_{n0}. Then it is this splitting that determines the interwell tunneling; it largely exceeds δg_0, but the effect becomes small when the relaxation rate exceeds h_{n0}.

For $\hbar\omega_F \sim \Delta U$, one should take into account transitions $\psi_0^{(l,r)} \to \psi_n$ via intermediate states, which appear in higher-order in $\hat{h}$. From Eq. (12), if the intermediate states are arranged in the order of increasing quasienergies, the resulting transition matrix elements have the same exponent as h_{n0}. Thus the corresponding virtual processes just renormalize the prefactor in the resonant tunnel splitting compared to Eq. (12). The shift of the dimensionless quasienergy levels g_n due to the term $\hat{h}(t)$ in the Hamiltonian is $\sim\omega_{\mathrm{sl}}/\omega_F$. It does not contain an exponentially small factor, smoothly depends on n, and largely exceeds h_{n0}.

Figure 3 shows extremely sharp resonant peaks of the splitting of quasienergy levels for $\hbar\omega_F$ resonating with the renormalized interlevel distance $(F^2/6\gamma)(g_n - g_0)$. Instead of calculating this distance and the prefactor in h_{n0} to high order in $\hat{h}$ we used them as adjustable parameters when comparing numerical results with Eq. (12).

Even moderately weak relaxation modifies the interwell transitions if the oscillator decay rate Γ exceeds the tunneling frequency $\omega_{\mathrm{sl}}\nu_-$. We will consider the resonant case, where the dimensionless decay rate $\kappa = \Gamma/\omega_{\mathrm{sl}} \ll 1$ but $\kappa \gg \Delta$. If $\kappa \gg h_{n0}/\lambda$, resonant transitions $\psi_0^{(l,r)} \to \psi_n$ occur at dimensionless rate $\sim h_{n0}^2/\lambda^2\kappa$. From the resonantly excited state ψ_n the system drifts down in quasienergy and approaches the states $\psi_0^{(l)}$ and $\psi_0^{(r)}$ with equal probabilities. As a result, instead of tunneling the system incoherently switches between the wells with rate $\sim h_{n0}^2/\lambda^2\kappa$, see Supplemental Material [15].

Relaxation leads to interwell switching on its own via the mechanism of quantum activation [8,10]. The dimensionless switching rate is $\nu_{QA} \sim \kappa \exp(-R_A/\lambda)$. From the explicit form of the activation exponent R_A [8] and Eq. (12), it follows that, for $T = 0$, the rate $h_{n0}^2/\lambda^2\kappa$ is exponentially higher than the quantum activation rate for $\mu \gtrsim -0.35$, if the resonant quasienergy level is near the barrier top, $|g_n| \lesssim \lambda$. For T exceeding a small μ- and κ-dependent threshold value (still $T \ll \hbar\omega_F/2k_B$), R_A becomes smaller than the leading-order term in $2\lambda|\ln h_{n0}|$. The difference between these quantities quickly falls down with increasing μ, and for realistic not too small λ and small quantum activation prefactor κ, the $\hat{h}$-field induced switching may still dominate at resonance.

In conclusion, we have found a new mechanism of transitions between coexisting vibrational states of a parametric oscillator. The transitions correspond to resonant tunneling in a Λ-type configuration of quasienergy states and come from the terms, which are conventionally disregarded in the RWA. The transition amplitude is found using the conformal mapping technique. It displays sharp resonant peaks as a function of the modulation frequency and at its maxima is exponentially larger than the RWA tunneling amplitude. The peaks should make it possible to observe the effect in experiments on oscillators with a high quality factor, including the currently studied Josephson junction based oscillators [1].

The research of V. P and M. I. D was supported in part by the NSF, Grant No. EMT/QIS 082985.

[1] R. Vijay, M. H. Devoret, and I. Siddiqi, Rev. Sci. Instrum. **80**, 111101 (2009); F. Mallet, F. R. Ong, A. Palacios-Laloy, F. Nguyen, P. Bertet, D. Vion, and D. Esteve, Nature Phys. **5**, 791 (2009); C. M. Wilson, T. Duty, M. Sandberg, F. Persson, V. Shumeiko, and P. Delsing, Phys. Rev. Lett. **105**, 233907 (2010).
[2] G. J. Walls and D. F. Milburn, *Quantum Optics* (Springer, Berlin, 2008).
[3] S. Peil and G. Gabrielse, Phys. Rev. Lett. **83**, 1287 (1999).
[4] T. J. Kippenberg and K. J. Vahala, Science **321**, 1172 (2008); F. Brennecke, S. Ritter, T. Donner, and T. Esslinger, Science **322**, 235 (2008); A. A. Clerk, F. Marquardt, and J. G. E. Harris, Phys. Rev. Lett. **104**,

213603 (2010); T. P. Purdy, D. W. C. Brooks, T. Botter, N. Brahms, Z.-Y. Ma, and D. M. Stamper-Kurn, Phys. Rev. Lett. **105**, 133602 (2010); J. Chan, T. P. M. Alegre, A. H. Safavi-Naeini, J. T. Hill, A. Krause, S. Gröblacher, M. Aspelmeyer, and O. Painter, Nature (London) **478**, 89 (2011).

[5] M. J. Davis and E. J. Heller, J. Chem. Phys. **75**, 246 (1981).

[6] L. D. Landau and E. M. Lifshitz, *Mechanics* (Elsevier, Amsterdam, 2004), 3rd ed..

[7] B. Wielinga and G. J. Milburn, Phys. Rev. A **48**, 2494 (1993).

[8] M. Marthaler and M. I. Dykman, Phys. Rev. A **73**, 042108 (2006); **76**, 010102R (2007).

[9] P. D. Drummond and D. F. Walls, J. Phys. A **13**, 725 (1980); P. Kinsler and P. D. Drummond, Phys. Rev. A **43**, 6194 (1991).

[10] M. I. Dykman and V. N. Smelyansky, Zh. Eksp. Teor. Fiz. **94**, 61 (1988).

[11] V. N. Sazonov and V. I. Finkelstein, Dokl. Akad. Nauk SSSR **231**, 78 (1976); A. P. Dmitriev and M. I. Dyakonov, Zh. Eksp. Teor. Fiz. **90**, 1430 (1986); K. Vogel and H. Risken, Phys. Rev. A **38**, 2409 (1988); V. Peano and M. Thorwart, Phys. Rev. B **70**, 235401 (2004); I. Serban and F. K. Wilhelm, Phys. Rev. Lett. **99**, 137001 (2007).

[12] E. Lucero, M. Hofheinz, M. Ansmann, R. C. Bialczak, N. Katz, M. Neeley, A. D. O'Connell, H. Wang, A. N. Cleland, and J. M. Martinis, Phys. Rev. Lett. **100**, 247001 (2008).

[13] O. Bohigas, S. Tomsovic, and D. Ullmo, Phys. Rep. **223**, 43 (1993); W. K. Hensinger *et al.*, Nature (London) **412**, 52 (2001); D. A. Steck, W. H. Oskay, and M. G. Raizen, Science **293**, 274 (2001).

[14] O. Brodier, P. Schlagheck, and D. Ullmo, Phys. Rev. Lett. **87**, 064101 (2001); O. Brodier, P. Schlagheck, and D. Ullmo, Ann. Phys. (N.Y.) **300**, 88 (2002); S. Lock, A. Bäcker, R. Ketzmerick, and P. Schlagheck, Phys. Rev. Lett. **104**, 114101 (2010).

[15] See Supplemental Material at http://link.aps.org/supplemental/10.1103/PhysRevLett.109.090401 for the analysis of the classical trajectories, the conformal mapping from the coordinate to the complex time plane, and the evaluation of the prefactor in the WKB matrix elements. Also discussed there is the distinction of the quantum resonances in a weakly nonlinear oscillator from chaos- and resonance-assisted tunneling and the effects of dissipation.

[16] L. D. Landau and E. M. Lifshitz, *Quantum Mechanics. Non-Relativistic Theory* (Butterworth-Heinemann, Oxford, 1997), 3rd ed.